

A predictor-corrector deep learning algorithm for high dimensional stochastic partial differential equations

He Zhang ^{*1}, Ran Zhang^{†1}, and Tao Zhou^{‡2}

¹ School of Mathematics, Jilin University, Changchun, Jilin 130012, China

²Institute of Computational Mathematics and Scientific/Engineering Computing, Academy of Mathematics and Systems Science, Chinese Academy of Sciences, Beijing, 100190, China

September 13, 2022

Abstract

In this paper, we present a deep learning-based numerical method for approximating high dimensional stochastic partial differential equations (SPDEs). At each time step, our method relies on a predictor-corrector procedure. More precisely, we decompose the original SPDE into a degenerate SPDE and a deterministic PDE. Then in the prediction step, we solve the degenerate SPDE with the Euler scheme, while in the correction step we solve the second-order deterministic PDE by deep neural networks via its equivalent backward stochastic differential equation (BSDE). Under standard assumptions, error estimates and the rate of convergence of the proposed algorithm are presented. The efficiency and accuracy of the proposed algorithm are illustrated by numerical examples.

Keywords: Stochastic partial differential equations, deep learning, BSDEs.

AMS subject classifications: 60H15, 60H35, 65M12

^{*}Email: he_zhang@jlu.edu.cn. The work of this author was supported in part by NSFC Grant 12201242.

[†]Email: zhangran@jlu.edu.cn. Corresponding author. The work of this author was supported in part by NSFC Grant 11971198

[‡]Email: tzhou@lsec.cc.ac.cn. The work of this author was supported in part by NSFC Grants 11731006, 11831010 and 11871068.

1 Introduction

This paper is concerned with numerical methods for the following stochastic partial differential equation (SPDE):

$$\begin{aligned} u(t, x) = & h(x) + \int_t^T (\mathcal{L}u(s, x) + f(s, x, u(s, x), (\nabla u \sigma)(s, x))) \, ds \\ & + \int_t^T g(s, x, u(s, x)) \, dB_s, \end{aligned} \quad (1.1)$$

where $u: [0, T] \times \mathbb{R}^d \rightarrow \mathbb{R}^k$, $\mathcal{L}u = [Lu_1, \dots, Lu_k]^\top$ with

$$L = \frac{1}{2} \sum_{i,j=1}^d (\sigma \sigma^*)_{ij}(t, x) \frac{\partial^2}{\partial x_i \partial x_j} + \sum_{i=1}^d \mu_i(t, x) \frac{\partial}{\partial x_i}.$$

Here ∇ denotes the space gradient, B is a Brownian motion defined on some complete probability space (Ω, \mathcal{F}, P) , and the stochastic integral dB is a backward Itô integral. SPDEs of this type appear in many real-world applications such as filtering problems, population genetics, and statistical hydromechanics (see e.g. [43] and the references therein).

Numerical algorithms for the above SPDEs have been studied extensively in recent years. A comprehensive review of the literature can be found in Jentzen and Kloeden [38]. For low dimensional problems, traditional space-time concretization strategies can be adopted to obtain reasonable numerical accuracy, and this includes the finite difference methods [28, 29, 59], finite element methods [22, 57], spectral methods [26], and Wiener chaos decomposition [45], just to name a few. However, for higher dimensional problems, all these numerical approaches are infeasible due to their prohibitive computational costs and storage requirements (i.e., the so called curse of dimensionality). Consequently, probabilistic methods have been developed in recent years to mitigate the curse of dimensionality. An important starting point for designing probabilistic methods is due to Pardoux and Peng [51], in which they presented a probabilistic representation of the solution of (1.1) through the solution of the following forward backward doubly stochastic differential equation (FBDSDE)

$$X_s^{t,x} = x + \int_t^s \mu(r, X_r^{t,x}) \, dr + \int_t^s \sigma(r, X_r^{t,x}) \, dW_r, \quad (1.2)$$

$$\begin{aligned} Y_s^{t,x} = & h(X_T^{t,x}) + \int_s^T f(r, X_r^{t,x}, Y_r^{t,x}, Z_r^{t,x}) \, dr \\ & - \int_s^T Z_r^{t,x} \, dW_r + \int_s^T g(r, X_r^{t,x}, Y_r^{t,x}) \, dB_r, \end{aligned} \quad (1.3)$$

where $\{X_s^{t,x}, t \leq s \leq T\}$ denotes the forward process starting from x at time t , W is a d -dimensional standard Brownian motion independent of B in (1.1) and (1.3). More precisely, it was shown in [51] that if u is a classical solution

of (1.1), then $\{(Y_s^{t,x} = u(s, X_s^{t,x}), Z_s^{t,x} = (\nabla u \sigma)(s, X_s^{t,x})), t \leq s \leq T\}$ is the unique solution of (1.3). Based on this, various numerical methods for SPDEs using the associated FBDSDEs are proposed [2, 3, 5, 33]. In particular, when g vanishes, the above FBDSDEs become the so called backward stochastic differential equations (BSDEs), for which extensive numerical algorithms have been investigated [11, 20, 23, 24, 25, 58, 60, 61]. Nevertheless, designing efficient algorithms for high dimensional problems is still very challenging.

More recently, deep learning-based numerical methods have attracted great attention for dealing with high dimensional problems. In particular, E et al [14, 30] presented a deep leaning method for high-dimensional parabolic PDEs by using the nonlinear Feynman-Kac formula [50]. This approach was extended to fully nonlinear second-order PDEs in [7]. Backward induction schemes for high dimensional PDEs and variational inequalities were developed in [35]. A multi-level Picard iteration scheme was derived in [18] by combining the Feynman-Kac and Bismut-Elworthy-Li formulae with a multilevel Picard approximation.

Although there has been extensive research on deep learning-based numerical approximations for PDEs [15, 19, 34, 53, 55], however, very little attention has been paid to SPDEs. One can refer to [6] for numerical attempts on approximating solutions of initial value problems of SPDEs by neural networks. We also mention the work of Teng et al [56] on deep learning-based numerical scheme for FBDSDEs, where they define equivalent control problems by treating Y_t and Z_t in FBDSDE as controls, and use deep neural networks as approximation tools for these controls.

In this work, we shall present a predictor-corrector (or, an operator splitting) deep learning scheme for the weak solution of (1.1). Consider the following partition of $[0, T]$:

$$\pi^N: 0 = t_0 < t_1 < \cdots < t_N = T.$$

Our approach generates an approximated sequence $\{u_i(x)\}_{i=0}^N$ defined by

$$u_N = h(x), \quad u_i = \Phi_{\Delta t_i} \Psi_{t_i, t_{i+1}} u_{i+1}, \quad i = N-1, \dots, 0, \quad (1.4)$$

where $\Delta t_i = t_{i+1} - t_i$, $\{\Phi_t, t \geq 0\}$ and $\{\Psi_{st}, 0 \leq s \leq t\}$ denote the solution operators associated with the equations

$$d\psi + g(t, x, \psi(t, x)) dB_t = 0, \quad \lim_{t \uparrow t_{i+1}} \psi_t = u_{i+1} = \varphi_{t_{i+1}}, \quad (1.5)$$

and

$$\partial_t \varphi + \mathcal{L}\varphi(t, x) + f(t, x, \varphi(t, x), (\nabla \varphi \sigma)(t, x)) = 0, \quad \lim_{t \uparrow t_{i+1}} \varphi_t = \psi_{t_i}, \quad (1.6)$$

respectively. Notice that at each time step, the SDE (1.5) serves as a predictor by providing an *a priori* estimate of the solution at the next time step. Then we adopt its solution at t_i as the terminal condition at t_{i+1} of the PDE (1.6), and refine the initial estimate. Consequently, $u_i(x) = \varphi_{t_i}(x)$ is an approximation of the solution $u(t_i, X_{t_i}^{t,x})$. We employ the Euler scheme for the SDE (1.5), and the numerical approximation of the PDE (1.6) is of primary interest. Inspired

by [14, 30], we shall propose to approximate (1.6) by a deep neural network at each time step via its equivalent BSDE. Besides proposing the splitting scheme, our second contribution shall be the sharp convergence analysis of the proposed algorithm.

The main motivation for proposing the above splitting strategy is that it not only improves efficiency, but also provides remarkable flexibility in choosing different numerical methods for each sub-problem. Similar splitting ideas for linear SPDEs such as the Zakai equation have been discussed in [8, 9, 11, 27, 44, 49].

The rest of the paper is organized as follows. In section 2, we provide with some preliminaries and present the discrete time approximation scheme for (1.1) and its error estimates. In section 3, we present the deep learning algorithm based on the discrete time approximations in section 2. The convergence analysis of the proposed algorithm and the error estimates in terms of the approximation errors of the neural networks will also be presented. Numerical examples are presented in Section 4, and this is followed by some concluding remarks in Section 5.

2 Preliminaries

Throughout the paper, we denote by (Ω, \mathcal{F}, P) a probability space on which two mutually independent standard Brownian motions W and B (with values in \mathbb{R}^d and \mathbb{R}^l , respectively) are defined. Let $\mathcal{F}_{s,t}^W$ and $\mathcal{F}_{s,t}^B$ be the usual P-augmentation of $\sigma\{W_r - W_s; s \leq r \leq t\}$ and $\sigma\{B_r - B_s; s \leq r \leq t\}$, respectively. For each $t \in [0, T]$, we define two collections $\{\mathcal{F}_t\}_{0 \leq t \leq T}$ and $\{\mathcal{G}_t\}_{0 \leq t \leq T}$ by

$$\mathcal{F}_t := \mathcal{F}_{0,t}^W \vee \mathcal{F}_{t,T}^B, \text{ and } \mathcal{G}_t := \mathcal{F}_{0,t}^W \vee \mathcal{F}_{0,T}^B.$$

Note that $\{\mathcal{F}_t\}_{0 \leq t \leq T}$ is neither increasing nor decreasing, while $\{\mathcal{G}_t\}_{0 \leq t \leq T}$ is an increasing filtration. We also denote by $|x| = (\sum_{i=1}^n |x_i|^2)^{1/2}$ the Euclidean norm of a vector $x \in \mathbb{R}^n$ and by $|A| = (\sum_i \sum_j |a_{ij}|^2)^{1/2}$ the Frobenius norm for a matrix $A \in \mathbb{R}^{m \times n}$. Moreover, the following functional spaces will be frequently used:

- $C^k(\mathbb{R}^m; \mathbb{R}^n)$: the space of C^k -functions from \mathbb{R}^m to \mathbb{R}^n ;
- $C_c^k(\mathbb{R}^m; \mathbb{R}^n)$: the space of compactly supported C^k -functions;
- $C_b^k(\mathbb{R}^m; \mathbb{R}^n)$: the space of all C^k -functions whose partial derivatives up to order k are bounded.
- $L_{\mathcal{F}}^p(0, T; \mathbb{R}^n) (1 \leq p < \infty)$: the space of all \mathcal{F}_t -measurable \mathbb{R}^n -valued processes $\varphi(\cdot)$ such that

$$\mathbb{E} \left[\int_0^T |\varphi_t|^p dt \right] < \infty.$$

- $L_{\mathcal{F}}^p(\Omega, C([0, T]; \mathbb{R}^n))$: the space of all \mathcal{F}_t -measurable \mathbb{R}^n -valued continuous processes $\varphi(\cdot)$ such that

$$\mathbb{E} \left[\sup_{0 \leq t \leq T} |\varphi_t|^p \right] < \infty.$$

- $L_{\omega}^2(\mathbb{R}^n)$: a weighted Hilbert space with scalar product

$$(u, v)_{\omega} = \int_{\mathbb{R}^n} u(x)v(x)\omega(x) \, dx,$$

for which the induced norm yields $|u|_{\omega}^2 := (u, u)_{\omega}$. Here $\omega(x)$ is a continuous positive function such that $\int_{\mathbb{R}^n} (1 + |x|^2)\omega(x) \, dx < \infty$.

- $H_{\omega}^k(\mathbb{R}^n) (k \geq 0)$: the completion of $C_c^{\infty}(\mathbb{R}^n)$ with respect to the norm $|u|_{k, \omega}^2 = \sum_{0 \leq |\alpha| \leq k} |D^{\alpha} u|_{\omega}^2$.
- \mathcal{H} : the space of $\mathcal{F}_{t, T}^B$ -measurable process $\varphi_t(\cdot)$ with values in $H_{\omega}^1(\mathbb{R}^n)$ such that

$$|\varphi|_{\mathcal{H}}^2 := \mathbb{E} \left[\sup_{0 \leq t \leq T} |\varphi_t|_{\omega}^2 \right] + \mathbb{E} \left[\int_0^T |\nabla \varphi \sigma|_{\omega}^2 \, dt \right] < \infty.$$

In what follows, we also make the following assumptions.

- **(H1)** The functions f and g are jointly measurable in (t, x, y, z) such that $f(\cdot, \cdot, y, z) \in L_{\mathcal{F}}^2(0, T; \mathbb{R}^k)$ and $g(\cdot, \cdot, y) \in L_{\mathcal{F}}^2(0, T; \mathbb{R}^{k \times l})$. Furthermore, we assume that there exists a constant $K > 0$ such that

$$\begin{aligned} \sup_{0 \leq t \leq T} \left(|f(t, 0, 0, 0)|^2 + |g(t, 0, 0)|^2 \right) &\leq K, \\ |f(t, x, y, z) - f(s, \bar{x}, \bar{y}, \bar{z})|^2 + |g(t, x, y) - g(s, \bar{x}, \bar{y})|^2 \\ &\leq K (|t - s| + |x - \bar{x}|^2 + |y - \bar{y}|^2 + |z - \bar{z}|^2) \end{aligned}$$

for any $t, s \in [0, T]$, $x, \bar{x} \in \mathbb{R}^d$, $y, \bar{y} \in \mathbb{R}^k$, $z, \bar{z} \in \mathbb{R}^{k \times d}$.

- **(H2)** The terminal condition $h \in C_b^2(\mathbb{R}^d; \mathbb{R}^k)$ satisfies the following Lipschitz condition

$$|h(x) - h(\bar{x})|^2 \leq K|x - \bar{x}|^2, \quad \forall x, \bar{x} \in \mathbb{R}^d.$$

- **(H3)** The functions $\mu \in C_b^2(\mathbb{R}^d; \mathbb{R}^d)$ and $\sigma \in C_b^2(\mathbb{R}^d; \mathbb{R}^{d \times d})$ in (1.2) are uniformly $\frac{1}{2}$ -Hölder continuous in $t \in [0, T]$ and uniformly Lipschitz continuous in $x \in \mathbb{R}^d$, i.e., there exists a $K > 0$ such that

$$|\mu(t, x) - \mu(s, \bar{x})|^2 + |\sigma(t, x) - \sigma(s, \bar{x})|^2 \leq K (|t - s| + |x - \bar{x}|^2), \quad \forall x, \bar{x} \in \mathbb{R}^d.$$

Furthermore we assume that there exists a constant $c > 0$, such that

$$\xi^T \sigma(t, x) \sigma^T(t, x) \xi \geq c|\xi|^2, \quad \forall x, \xi \in \mathbb{R}^d, \quad t \in [0, T].$$

Under the above assumptions, it was shown in Pardoux and Peng [51] that the BDSDE (1.3) admits a unique solution

$$(Y, Z) \in L^2_{\mathcal{F}}(\Omega, C([0, T]; \mathbb{R}^k)) \times L^2_{\mathcal{F}}(0, T; \mathbb{R}^{k \times d}).$$

We are now ready to introduce the following definition

Definition 2.1 ([4]). A function $u \in \mathcal{H}$ is called a weak solution of (1.1) if for every $\phi \in C_c^\infty([0, T] \times \mathbb{R}^d)$, it holds

$$\begin{aligned} & \int_t^T \int_{\mathbb{R}^d} u(s, x) \partial_s \phi(s, x) dx ds - \int_t^T \int_{\mathbb{R}^d} u(s, x) \mathcal{L}^* \phi(s, x) dx ds \\ & + \int_{\mathbb{R}^d} u(t, x) \phi(t, x) dx - \int_{\mathbb{R}^d} h(x) \phi(T, x) dx \\ & = \int_t^T \int_{\mathbb{R}^d} f(s, x, u(s, x), (\nabla u \sigma)(s, x)) \phi(s, x) dx ds + \int_t^T \int_{\mathbb{R}^d} g(s, x, u(s, x)) \phi(s, x) dx dB_s, \end{aligned}$$

where \mathcal{L}^* is the adjoint of \mathcal{L} .

We close this section by recalling the following wellposedness and regularity results on BDSDEs.

Proposition 2.2 ([2, 4]). Under the assumptions **(H1)**-(**H3**), there exists a unique weak solution $u \in \mathcal{H}$ of the SPDE (1.1). Moreover, $u(t, x) = Y_t^{t,x}$, where $(Y_s^{t,x}, Z_s^{t,x})_{t \leq s \leq T}$ is the solution of the BDSDE (1.3). Furthermore, we have for all $s \in [t, T]$:

$$Y_s^{t,x} = u(s, X_s^{t,x}), \quad Z_s^{t,x} = (\nabla u \sigma)(s, X_s^{t,x}).$$

Proposition 2.3 ([2, 5, 51]). Let **(H1)**-(**H3**) hold. Then, for $0 \leq r \leq s \leq T$, there exists a positive constant C such that

$$\begin{aligned} E|Y_s^{t,x} - Y_r^{t,x}|^2 &\leq C(1 + |x|^2)(s - r), \\ E|Z_s^{t,x} - Z_r^{t,x}|^2 &\leq C(1 + |x|^2)(s - r). \end{aligned}$$

3 A predictor-corrector deep learning algorithm

In this section, based on predictor-corrector procedure (1.5)-(1.6), we shall present our predictor-corrector deep learning algorithm. To this end, we shall first discuss the temporal semi-discretizations and its error estimates, and then present the deep learning algorithm in the physical domain.

3.1 Temporal semi-discretizations

We first construct the discrete time approximations of the solution ψ in (1.5) and the solution φ in (1.6), to obtain the approximating sequence $\{u_i(x)\}_{i=0}^N$ defined in (1.4). We begin with the approximation of SDE (1.5). We recall the partition of $[0, T]$:

$$\pi^N: 0 = t_0 < t_1 < \cdots < t_N = T.$$

We further define the maximum partition size by $|\pi| := \max_i \Delta t_i$. The Euler scheme for (1.5) yields

$$\psi_{t_i}^\pi = \varphi_{t_{i+1}}^\pi + g\left(t_{i+1}, X_{t_{i+1}}^\pi, \varphi_{t_{i+1}}^\pi\right) \Delta B_i, \quad (3.1)$$

where $\varphi_{t_{i+1}}^\pi$ and $X_{t_{i+1}}^\pi$ are approximations of $\varphi(t, x)$ and X_t at $t = t_{i+1}$ which will be clarified later. In each interval $[t_i, t_{i+1})$, the PDE (1.6) is solved via its equivalent BSDE

$$y_s^{t,x} = \psi_{t_i}(x) + \int_s^{t_{i+1}} f(r, X_r^{t,x}, y_r^{t,x}, z_r^{t,x}) dr - \int_s^{t_{i+1}} z_r^{t,x} dW_r, \quad t_i \leq s < t_{i+1}. \quad (3.2)$$

It should be noted that the family $\{(y, z)\}$ differs from $\{(Y, Z)\}$ in (1.3), and y is discontinuous at points t_i . We recall Theorem 3.2 in [50] that shows

$$\varphi(t, x) = y_t^{t,x} \quad \text{and} \quad \nabla \varphi(t, x) \sigma(t, x) = z_t^{t,x}. \quad (3.3)$$

For this BSDE, we approximate the forward process X_t by the Euler scheme

$$X_{t_{i+1}}^{t,x,\pi} = X_{t_i}^{t,x,\pi} + \mu(t_i, X_{t_i}^{t,x,\pi}) \Delta t_i + \sigma(t_i, X_{t_i}^{t,x,\pi}) \Delta W_i, \quad (3.4)$$

Hereafter, the superscript t, x will be dropped unless clarity is needed. For the above scheme, the following estimate holds (see, e.g., [38]).

Lemma 3.1. *Assume that μ and σ satisfy **(H3)**. Then there exists a constant C , independent of π , such that*

$$\max_{0 \leq i \leq N-1} \sup_{s \in [t_i, t_{i+1})} \mathbb{E} \left[|X_s - X_{t_i}^\pi|^2 + |X_s - X_{t_{i+1}}^\pi|^2 \right] < C(1 + |x|^2) |\pi|.$$

Next, the solution (y, z) of (3.2) at $t = t_i$ is approximated by the solution $(y_{t_i}^\pi, z_{t_i}^\pi)$ via the following equation:

$$y_{t_i}^\pi = \psi_{t_i}^\pi + f(t_i, X_{t_i}^\pi, y_{t_i}^\pi, z_{t_i}^\pi) \Delta t_i - z_{t_i}^\pi \Delta W_i. \quad (3.5)$$

Notice that the scheme in (3.5) is implicit for y and z . Thus, by (3.3), $\varphi(t_i, \cdot)$ is approximated by

$$\varphi_{t_i}^\pi = y_{t_i}^\pi.$$

To sum up, given $\{(X_{t_i}^\pi, y_{t_i}^\pi, z_{t_i}^\pi)\}_{i=0}^N$, the solution ψ and φ of (1.5) and (1.6) is approximated by $\{\psi_{t_i}^\pi\}_{i=0}^N$ and $\{\varphi_{t_i}^\pi\}_{i=0}^N$, respectively, defined in a backward manner by $\varphi_{t_N}^\pi = h(X_{t_N}^\pi)$, and

$$\begin{aligned} \psi_{t_i}^\pi &= \varphi_{t_{i+1}}^\pi + g(t_{i+1}, X_{t_{i+1}}^\pi, \varphi_{t_{i+1}}^\pi) \Delta B_i, \\ \varphi_{t_i}^\pi &= y_{t_i}^\pi. \end{aligned} \quad (3.6)$$

Notice that the approximate sequence $\{u_i\}_{i=0}^N$ in (1.4) is defined by

$$u_i(x) = \varphi_{t_i}^\pi(x), \quad i = N-1, \dots, 0. \quad (3.7)$$

3.2 Error estimations of temporal semi-discretizations

In this section, we analyze the approximation error of the discrete time scheme described in Section 3.1. We first investigate the numerical error between the solution of BDSDE (1.3) and the discrete time scheme (3.5). To begin, we first present the following proposition.

Proposition 3.2. Suppose that **(H1)**-(**H3**) hold. Then there exists a constant C , independent of π , k , l , and the space dimension d , such that

$$\max_{0 \leq i \leq N-1} \mathbb{E}|Y_{t_i}^{t_i, \cdot} - y_{t_i}^\pi|^2 \leq C(1 + |x|^2)|\pi|. \quad (3.8)$$

Proof. Let $\mathbb{E}_i[\cdot]$ be the conditional expectation with respect to the discrete filtration $\mathcal{G}_{t_i}^\pi$ defined by

$$\mathcal{G}_{t_i}^\pi := \sigma\{\Delta W_j; 0 \leq j \leq i-1\} \vee \sigma\{\Delta B_j; 0 \leq j \leq N-1\}.$$

Setting $s = t_i$, taking the conditional expectation $\mathbb{E}_i[\cdot]$ in (1.3) and using the tower property, we have

$$\begin{aligned} Y_{t_i} &= \mathbb{E}_i \left[h(X_T) + \int_{t_i}^T f(r, X_r, Y_r, Z_r) dr + \int_{t_i}^T g(r, X_r, Y_r) dB_r \right] \\ &= \mathbb{E}_i \left[Y_{t_{i+1}} + \int_{t_i}^{t_{i+1}} f(r, X_r, Y_r, Z_r) dr + \int_{t_i}^{t_{i+1}} g(r, X_r, Y_r) dB_r \right]. \end{aligned} \quad (3.9)$$

We now define

$$\Delta y_i := Y_{t_i} - y_{t_i}^\pi (= Y_{t_i} - \varphi_{t_i}^\pi), \quad \Delta z_i := Z_{t_i} - z_{t_i}^\pi, \quad i = 0, \dots, N-1.$$

Then, by (3.9), (3.5) and (3.1), we have

$$\begin{aligned} \Delta y_i &= \mathbb{E}_i[Y_{t_{i+1}} - \psi_{t_i}^\pi] + \mathbb{E}_i \left[\int_{t_i}^{t_{i+1}} \delta f^i(r) dr \right] + \mathbb{E}_i \left[\int_{t_i}^{t_{i+1}} g(r, X_r, Y_r) dB_r \right] \\ &= \mathbb{E}_i[\Delta y_{i+1}] + \mathbb{E}_i \left[\int_{t_i}^{t_{i+1}} \delta f^i(r) dr \right] + \mathbb{E}_i \left[\int_{t_i}^{t_{i+1}} \delta g^{i+1}(r) dB_r \right], \end{aligned}$$

where

$$\begin{aligned} \delta f^i(r) &:= f(r, X_r, Y_r, Z_r) - f(t_i, X_{t_i}^\pi, y_{t_i}^\pi, z_{t_i}^\pi), \\ \delta g^{i+1}(r) &:= g(r, X_r, Y_r) - g(t_{i+1}, X_{t_{i+1}}^\pi, y_{t_{i+1}}^\pi). \end{aligned}$$

By squaring and then taking the expectation on both sides of the above equation

we obtain

$$\begin{aligned}\mathbb{E}|\Delta y_i|^2 &= \mathbb{E}|\mathbb{E}_i[\Delta y_{i+1}]|^2 + \mathbb{E}\left|\int_{t_i}^{t_{i+1}} \mathbb{E}_i[\delta f^i(r)] \, dr\right|^2 + \mathbb{E}\left|\mathbb{E}_i\left[\int_{t_i}^{t_{i+1}} \delta g^{i+1}(r) \, dB_r\right]\right|^2 \\ &\quad + 2\mathbb{E}\left[\mathbb{E}_i[\Delta y_{i+1}] \int_{t_i}^{t_{i+1}} \mathbb{E}_i[\delta f^i(r)] \, dr\right] + 2\mathbb{E}\left[\mathbb{E}_i[\Delta y_{i+1}] \mathbb{E}_i\left[\int_{t_i}^{t_{i+1}} \delta g^{i+1}(r) \, dB_r\right]\right] \\ &\quad + 2\mathbb{E}\left[\int_{t_i}^{t_{i+1}} \mathbb{E}_i[\delta f^i(r)] \, dr \mathbb{E}_i\left[\int_{t_i}^{t_{i+1}} \delta g^{i+1}(r) \, dB_r\right]\right] := I_1 + I_2 + I_3 + I_4 + I_5 + I_6.\end{aligned}$$

By Cauchy's inequality, Jensen's inequality, and **(H1)**, we have

$$\begin{aligned}I_2 &\leq \Delta t_i \mathbb{E}\left[\int_{t_i}^{t_{i+1}} (\mathbb{E}_i[\delta f^i(r)])^2 \, dr\right] \\ &\leq K \Delta t_i \int_{t_i}^{t_{i+1}} (|r - t_i| + \mathbb{E}|X_r - X_{t_i}^\pi|^2 + \mathbb{E}|Y_r - y_{t_i}^\pi|^2 + \mathbb{E}|Z_r - z_{t_i}^\pi|^2) \, dr.\end{aligned}$$

Next, by Itô's isometry, Jensen's inequality, and **(H1)**, we obtain

$$\begin{aligned}I_3 &= \mathbb{E}\left[\int_{t_i}^{t_{i+1}} (\mathbb{E}_i[\delta g^{i+1}(r)])^2 \, dr\right] \\ &\leq K \int_{t_i}^{t_{i+1}} (|r - t_i| + \mathbb{E}|X_r - X_{t_{i+1}}^\pi|^2 + \mathbb{E}|Y_r - y_{t_{i+1}}^\pi|^2) \, dr.\end{aligned}$$

Notice that Y_s is $\mathcal{F}_{s,T}^B$ -measurable, Δy_{i+1} is $\mathcal{F}_{t_{i+1},T}^B$ -measurable, thus we have

$$\mathbb{E}\left[\mathbb{E}_i[\Delta y_{i+1}] \mathbb{E}_i\left[\int_{t_i}^{t_{i+1}} g(r, X_r, Y_r) - g(t_{i+1}, X_{t_{i+1}}, Y_{t_{i+1}}) \, dB_r\right]\right] = 0.$$

Consequently, by properties of the conditional expectations we obtain

$$I_5 = \mathbb{E}\left[\mathbb{E}_i[\Delta y_{i+1}] \mathbb{E}_i[\tilde{\delta} g^{i+1} \Delta B_i]\right] = 0,$$

where $\tilde{\delta} g^{i+1} = g(t_{i+1}, X_{t_{i+1}}, Y_{t_{i+1}}) - g(t_{i+1}, X_{t_{i+1}}^\pi, y_{t_{i+1}}^\pi)$. We next estimate I_4 and I_6 . It follows from Young's inequality, Jensen's inequality, and the estimates of I_2 and I_3 that

$$\begin{aligned}I_4 + I_6 &\leq \epsilon_1 \Delta t_i \mathbb{E}|\Delta y_{i+1}|^2 + \frac{1}{\epsilon_1 \Delta t_i} \mathbb{E}\left|\int_{t_i}^{t_{i+1}} \mathbb{E}_i[\delta f^i(r)] \, dr\right|^2 \\ &\quad + \frac{1}{\epsilon_2} \mathbb{E}\left|\int_{t_i}^{t_{i+1}} \mathbb{E}_i[\delta f^i(r)] \, dr\right|^2 + \epsilon_2 \mathbb{E}\left|\int_{t_i}^{t_{i+1}} \mathbb{E}_i[\delta g^{i+1}(r)] \, dB_r\right|^2 \\ &\leq \epsilon_1 \Delta t_i \mathbb{E}|\Delta y_{i+1}|^2 + \epsilon_2 K \int_{t_i}^{t_{i+1}} (|r - t_i| + \mathbb{E}|X_r - X_{t_{i+1}}^\pi|^2 + \mathbb{E}|Y_r - y_{t_{i+1}}^\pi|^2) \, dr \\ &\quad + \left(\frac{1}{\epsilon_1} + \frac{\Delta t_i}{\epsilon_2}\right) K \int_{t_i}^{t_{i+1}} (|r - t_i| \mathbb{E}|X_r - X_{t_i}^\pi|^2 + \mathbb{E}|Y_r - y_{t_i}^\pi|^2 + \mathbb{E}|Z_r - z_{t_i}^\pi|^2) \, dr.\end{aligned}$$

By Jensen's inequality, we have

$$\begin{aligned}\mathbb{E}|Y_r - y_{t_i}^\pi|^2 &\leq 2\mathbb{E}|\Delta y_i|^2 + 2\mathbb{E}|Y_r - Y_{t_i}|^2, \\ \mathbb{E}|Y_r - y_{t_{i+1}}^\pi|^2 &\leq 2\mathbb{E}|\Delta y_{i+1}|^2 + 2\mathbb{E}|Y_r - Y_{t_{i+1}}|^2, \\ \mathbb{E}|Z_r - z_{t_i}^\pi|^2 &\leq 2\mathbb{E}|\Delta z_i|^2 + 2\mathbb{E}|Z_r - Z_{t_i}|^2.\end{aligned}$$

Then, using together Proposition 2.3, Lemma 3.1, and **(H1)** we obtain

$$\begin{aligned}\mathbb{E}|\Delta y_i|^2 &\leq \mathbb{E}|\mathbb{E}_i[\Delta y_{i+1}]|^2 + \epsilon_1 \Delta t_i \mathbb{E}|\Delta y_{i+1}|^2 + 2K(1 + \epsilon_2) \Delta t_i \mathbb{E}|\Delta y_{i+1}|^2 \\ &\quad + 2K \left(\frac{1}{\epsilon_1} + \Delta t_i + \frac{\Delta t_i}{\epsilon_2} \right) (\Delta t_i) \mathbb{E}|\Delta y_i|^2 \\ &\quad + 2K \left(\frac{1}{\epsilon_1} + \Delta t_i + \frac{\Delta t_i}{\epsilon_2} \right) (\Delta t_i) \mathbb{E}|\Delta z_i|^2 + C(1 + |x|^2)(\Delta t_i)^2.\end{aligned}\tag{3.10}$$

Now we turn to the estimation of Δz_i . Setting $s = t_i$, multiplying (1.3) by ΔW_i , and taking the conditional expectation $\mathbb{E}_i[\cdot]$, we obtain by the integration by parts formula that

$$\begin{aligned}\Delta t_i Z_{t_i} &= \mathbb{E}_i[Y_{t_{i+1}} \Delta W_i] + \mathbb{E}_i \left[\int_{t_i}^{t_{i+1}} f(r, X_r, Y_r, Z_r) dr \Delta W_i \right] \\ &\quad + \mathbb{E}_i \left[\int_{t_i}^{t_{i+1}} g(r, X_r, Y_r) dB_r \Delta W_i \right] + \int_{t_i}^{t_{i+1}} \mathbb{E}_i[Z_{t_i} - Z_r] dr.\end{aligned}\tag{3.11}$$

Similarly, multiplying (3.5) by ΔW_i , taking the conditional expectation $\mathbb{E}_i[\cdot]$, and combining with (3.1), we get

$$\Delta t_i z_{t_i}^\pi = \mathbb{E}_i[\psi_{t_i}^\pi \Delta W_i] = \mathbb{E}_i \left[(\varphi_{t_{i+1}}^\pi + g(t_{i+1}, X_{t_{i+1}}^\pi, \varphi_{t_{i+1}}^\pi) \Delta B_i) \Delta W_i \right]. \tag{3.12}$$

Subtracting (3.12) from (3.11) gives

$$\begin{aligned}\Delta t_i \Delta z_i &= \mathbb{E}_i[\Delta y_{i+1} \Delta W_i] + \mathbb{E}_i \left[\int_{t_i}^{t_{i+1}} f(r, X_r, Y_r, Z_r) dr \Delta W_i \right] \\ &\quad + \mathbb{E}_i \left[\int_{t_i}^{t_{i+1}} \delta g^{i+1}(r) dB_r \Delta W_i \right] + \int_{t_i}^{t_{i+1}} \mathbb{E}_i[Z_{t_i} - Z_r] dr.\end{aligned}$$

We now square the above equation and take expectation to get

$$\begin{aligned}
\mathbb{E}|\Delta t_i \Delta z_i|^2 &= \mathbb{E} \left| \mathbb{E}_i[\Delta y_{i+1} \Delta W_i] \right|^2 \\
&\quad + \mathbb{E} \left[\left\{ \mathbb{E}_i \left[\int_{t_i}^{t_{i+1}} f(r, X_r, Y_r, Z_r) dr \Delta W_i \right] \right. \right. \\
&\quad \left. \left. + \mathbb{E}_i \left[\int_{t_i}^{t_{i+1}} \delta g^{i+1}(r) dB_r \Delta W_i \right] + \int_{t_i}^{t_{i+1}} \mathbb{E}_i[Z_{t_i} - Z_r] dr \right\}^2 \right] \\
&\quad + 2\mathbb{E} \left[\mathbb{E}_i[\Delta y_{i+1} \Delta W_i] \mathbb{E}_i \left[\int_{t_i}^{t_{i+1}} f(r, X_r, Y_r, Z_r) dr \Delta W_i \right] \right] \\
&\quad + 2\mathbb{E} \left[\mathbb{E}_i[\Delta y_{i+1} \Delta W_i] \mathbb{E}_i \left[\int_{t_i}^{t_{i+1}} \delta g^{i+1}(r) dB_r \Delta W_i \right] \right] \\
&\quad + 2\mathbb{E} \left[\mathbb{E}_i[\Delta y_{i+1} \Delta W_i] \int_{t_i}^{t_{i+1}} \mathbb{E}_i[Z_r - Z_{t_i}] dr \right] \\
&:= J_1 + J_2 + J_3 + J_4 + J_5.
\end{aligned}$$

We now estimate term by term. By Cauchy's inequality, Jensen's inequality, Itô's isometry, **(H1)**, Proposition 2.3, Lemma 3.1, and the estimate of I_3 , we have

$$\begin{aligned}
J_2 &\leq 3(\Delta t_i)^2 \int_{t_i}^{t_{i+1}} \mathbb{E}|f(r, X_r, Y_r, Z_r)|^2 dr \\
&\quad + 3\Delta t_i \int_{t_i}^{t_{i+1}} \mathbb{E}|\delta g^{i+1}(r)|^2 dr + 3\Delta t_i \int_{t_i}^{t_{i+1}} \mathbb{E}|Z_{t_i} - Z_r|^2 dr \\
&\leq 6K(\Delta t_i)^2 \mathbb{E}|\Delta y_{i+1}|^2 + C(1 + |x|^2)(\Delta t_i)^3.
\end{aligned}$$

Combining the above result with Young's inequality, we have

$$\begin{aligned}
J_3 &\leq \varepsilon_3 \mathbb{E} \left| \mathbb{E}_i[\Delta y_{i+1} \Delta W_i] \right|^2 + C(1 + |x|^2)(\Delta t_i)^3, \\
J_4 &\leq \varepsilon_4 \mathbb{E} \left| \mathbb{E}_i[\Delta y_{i+1} \Delta W_i] \right|^2 + \frac{1}{\varepsilon_4} \left[2K(\Delta t_i)^2 \mathbb{E}|\Delta y_{i+1}|^2 + C(1 + |x|^2)(\Delta t_i)^3 \right], \\
J_5 &\leq \varepsilon_5 \mathbb{E} \left| \mathbb{E}_i[\Delta y_{i+1} \Delta W_i] \right|^2 + C(1 + |x|^2)(\Delta t_i)^3.
\end{aligned}$$

Thus we have

$$\begin{aligned}
(\Delta t_i)^2 \mathbb{E}|\Delta z_i|^2 &\leq (1 + \varepsilon) \mathbb{E} \left| \mathbb{E}_i[\Delta y_{i+1} \Delta W_i] \right|^2 + C_z(\Delta t_i)^2 \mathbb{E}|\Delta y_{i+1}|^2 \\
&\quad + C(1 + |x|^2)(\Delta t_i)^3,
\end{aligned} \tag{3.13}$$

where $\varepsilon := \varepsilon_3 + \varepsilon_4 + \varepsilon_5$, and $C_z = 6K + \frac{2K}{\varepsilon_4}$. Now by Cauchy's inequality we have

$$\left| \mathbb{E}_i[\Delta y_{i+1} \Delta W_i] \right|^2 \leq \Delta t_i \left(\mathbb{E}_i[|\Delta y_{i+1}|^2] - |\mathbb{E}_i[\Delta y_{i+1}]|^2 \right). \tag{3.14}$$

Then plugging (3.14) and (3.13) into (3.10), we obtain

$$\begin{aligned} C_y^1 \mathbb{E} |\Delta y_i|^2 &\leq C_y^2 \mathbb{E} |\Delta y_{i+1}|^2 + (1 - C_y^2) \mathbb{E} \left| \mathbb{E}_i [\Delta y_{i+1}] \right|^2 \\ &\quad + C_y^3 \Delta t_i \mathbb{E} |\Delta y_{i+1}|^2 + C \left(1 + |x|^2 \right) (\Delta t_i)^2, \end{aligned} \quad (3.15)$$

where

$$\begin{aligned} C_y^1 &= 1 - 2K \left(\frac{1}{\epsilon_1} + \Delta t_i + \frac{\Delta t_i}{\epsilon_2} \right) (\Delta t_i), \quad C_y^2 = 2K \frac{1 + \varepsilon}{\epsilon_1}, \\ C_y^3 &= \varepsilon_1 + 2K(1 + \varepsilon_2) + 2K \left(1 + \frac{1}{\varepsilon_2} \right) (1 + \varepsilon) + 2K \left(\frac{1}{\epsilon_1} + \Delta t_i + \frac{\Delta t_i}{\epsilon_2} \right) C_z. \end{aligned}$$

With appropriately chosen $\varepsilon_1, \varepsilon_3, \varepsilon_4$, and ε_5 we may set $C_y^2 = 1$. Thus we obtain

$$\begin{aligned} \mathbb{E} |\Delta y_i|^2 &\leq (C_y^1)^{-1} \mathbb{E} \left| \Delta y_{i+1} \right|^2 + (C_y^1)^{-1} C_y^3 \Delta t_i \mathbb{E} \left| \Delta y_{i+1} \right|^2 + C \left(1 + |x|^2 \right) (\Delta t_i)^2 \\ &\leq \left(1 + C \Delta t_i \right) \mathbb{E} \left| \Delta y_{i+1} \right|^2 + C \left(1 + |x|^2 \right) (\Delta t_i)^2. \end{aligned} \quad (3.16)$$

Then, by applying the discrete Gronwall inequality and Lemma 3.1 to (3.16), we have

$$\max_{0 \leq i \leq N} \mathbb{E} |\Delta y_i|^2 \leq C(1 + |x|^2) |\pi|.$$

This completes the proof. \square

We now present the following theorem that shows the convergence of the time-discretization scheme.

Theorem 3.3. *Let (H1)-(H3) hold. Then there exists a constant C , independent of π, k, l , and the space dimension d , such that*

$$\max_{0 \leq i \leq N-1} \mathbb{E} \left| u(t_i, X_{t_i}^{t,x}) - u_i \right|_\omega^2 \leq C |\pi|.$$

Proof. It follows from Proposition 3.2 that

$$\begin{aligned} \mathbb{E} \left[\int_{\mathbb{R}^d} \left| u(t_i, X_{t_i}^{t,x}) - u_i(x) \right|^2 \omega(x) dx \right] &= \mathbb{E} \left[\int_{\mathbb{R}^d} \left| Y_{t_i}^{t_i, X_{t_i}^{t,x}} - y_i^\pi \right|^2 \omega(x) dx \right] \\ &\leq \int_{\mathbb{R}^d} \left(\max_{0 \leq i \leq N-1} \mathbb{E} \left| Y_{t_i}^{t_i, X_{t_i}^{t,x}} - y_i^\pi \right|^2 \right) \omega(x) dx \\ &\leq C |\pi| \int_{\mathbb{R}^d} \left(1 + |x|^2 \right) \omega(x) dx \leq C |\pi|. \end{aligned}$$

The proof is completed. \square

3.3 DNNs-approximations in the physical domain

In this section, we propose a deep learning-based numerical scheme for the discrete time approximations (3.6) and (3.7). To this end, we begin with a general review of how deep neural networks (DNNs) approximate unknown functions. Consider a feedforward neural network \mathcal{N}_{L+1} with $L + 1$ layers ($L > 1$). The input layer will be referred to as layer 0 and the output layer as layer L . The layers in between are called *hidden layers*. The basic building block of a neural network is an *artificial neuron* or *node*. Each input i_k has an associated weight w_k . For the sake of simplicity, the bias terms are not treated specially, as they correspond to a weight with a fixed input of 1. The sum of all weighted inputs, $S = \sum_k i_k w_k$, is passed through a nonlinear activation function σ , to transform the preactivation level of the neuron to an output $O = \sigma(\sum_k i_k w_k)$. The output O is used as an input by nodes in the next layer. Let n_l be the number of neurons on the l -th layer. For simplicity, we set $n_l = \bar{n}$, for $l = 1, \dots, L - 1$. Thus a feedforward neural network is a function defined as the composition

$$\mathcal{N}_{L+1}^{n_0, \bar{n}, n_L}(x_0, \mathcal{W}, \sigma_0, \dots, \sigma_L) := \sigma_L \circ S_L \circ \sigma_{L-1} \circ S_{L-1} \circ \dots \circ \sigma_0 \circ S_0(x_0),$$

where $x_0 \in \mathbb{R}^{n_0}$ is the network input, S_l and σ_l are the weighted sum and the activation function of the l -th layer, respectively. \mathcal{W} contains all the parameters (weights and biases) of the network. The dimension of \mathcal{W} is

$$n_{\mathcal{W}} = \sum_{l=1}^L n_l \times n_{l-1} + n_{l-1} = (n_0 + 1)\bar{n} + (\bar{n} + 1)\bar{n}(L - 1) + (\bar{n} + 1)n_L.$$

Recall the Euler method (3.4). For every fixed path $\{\Delta B_i, 0 \leq i \leq N - 1\}$ of the Brownian motion B , we approximate $\psi_{t_i}^\pi$ in (3.1) by

$$\psi_{t_i}^\pi \approx \Psi_i^*(X_{t_{i+1}}^\pi, \Delta B_i),$$

with

$$\Psi_i^*(X_{t_{i+1}}^\pi, \Delta B_i) = \mathcal{U}_{i+1}^*(X_{t_{i+1}}^\pi) + g\left(t_{i+1}, X_{t_{i+1}}^\pi, \mathcal{U}_{i+1}^*(X_{t_{i+1}}^\pi)\right) \Delta B_i, \quad (3.17)$$

where the notation $\mathcal{U}_{i+1}^*(X_{t_{i+1}}^\pi)$ will be explained later. For $i = N - 1, \dots, 0$, we approximate $y_{t_i}^\pi$ and $z_{t_i}^\pi$ in (3.5) by a pair of neural networks $\mathcal{U}_i(\cdot; \theta_i) \in \mathcal{N}_{L+1}^{d, \bar{n}, 1}$ and $\mathcal{V}_i(\cdot; \theta_i) \in \mathcal{N}_{L+1}^{d, \bar{n}, d}$ with parameter θ_i . Then, the optimal parameters θ_i^* are determined by minimizing the following loss function

$$\begin{aligned} L_i(\theta_i) = \mathbb{E} & \left| \Psi_i^*(X_{t_{i+1}}^\pi, \Delta B_i) - \mathcal{V}_i(X_{t_i}^\pi; \theta_i) \Delta W_i \right. \\ & \left. + f\left(t_i, X_{t_i}^\pi, \mathcal{U}_i(X_{t_i}^\pi; \theta_i), \mathcal{V}_i(X_{t_i}^\pi; \theta_i)\right) \Delta t_i - \mathcal{U}_i(X_{t_i}^\pi; \theta_i) \right|^2. \end{aligned}$$

We set

$$\mathcal{U}_i^*(X_{t_i}^\pi) = \mathcal{U}_i(X_{t_i}^\pi; \theta_i^*), \quad \mathcal{V}_i^*(X_{t_i}^\pi) = \mathcal{V}_i(X_{t_i}^\pi; \theta_i^*).$$

It follows from (3.6) that the value of the solution u of (1.1) at time t_i is approximated by $\mathcal{U}_i^*(X_{t_i}^\pi)$. We remark $\mathcal{V}_i^*(X_{t_i}^\pi)$ is not an approximation of $(\nabla u \sigma)$ at time t_i . In comparison to the global optimization problem formulated in [56], which requires to keep in memory all the computed network approximations of u , the memory requirements for our proposed algorithm are significantly reduced. We finally present the whole computational procedure in Algorithm 1.

Algorithm 1:

Data: Sample paths of $\{X_{t_i}^\pi\}_{i=0}^N$, $\{\Delta W_i\}_{i=0}^{N-1}$ and $\{\Delta B_i\}_{i=0}^{N-1}$

- 1 $\mathcal{U}_N^* = h(X_{t_N}^\pi)$.
- 2 **for** $i = N-1, \dots, 0$ **do**
- 3 Set $\Psi_i^*(X_{t_{i+1}}^\pi, \Delta B_i) = \mathcal{U}_{i+1}^*(X_{t_{i+1}}^\pi) + g(t_{i+1}, X_{t_{i+1}}^\pi, \mathcal{U}_{i+1}^*(X_{t_{i+1}}^\pi)) \Delta B_i$
- 4 Train a pair of deep neural networks $\mathcal{U}_i(X_{t_i}^\pi; \theta_i)$ and $\mathcal{V}_i(X_{t_i}^\pi; \theta_i)$ for the approximation of $(y_{t_i}^\pi, z_{t_i}^\pi)$ by minimizing $L_i(\theta_i)$. Set

$$\theta_i^* = \arg \min L_i(\theta_i).$$
- 5 Update $\mathcal{U}_i^*(X_{t_i}^\pi) = \mathcal{U}_i(X_{t_i}^\pi; \theta_i^*)$ and $\mathcal{V}_i^*(X_{t_i}^\pi) = \mathcal{V}_i(X_{t_i}^\pi; \theta_i^*)$.
- 6 $u(0, X_0) = Y_0^{0, X_0} \approx \mathcal{U}_0^*(X_{t_0}^\pi)$.

We now define

$$\mathcal{U}_{t_i}^\pi = \Psi_i^*(X_{t_{i+1}}^\pi, \Delta B_i) + f\left(t_i, X_{t_i}^\pi, \mathcal{U}_{t_i}^\pi, \mathcal{V}_{t_i}^\pi\right) \Delta t_i - \mathcal{V}_{t_i}^\pi \Delta W_i, \quad (3.18)$$

Then the following theorem presents the convergence result for the algorithm.

Theorem 3.4. *Assume that (H1)-(H3) hold. We also suppose that the partition π satisfies the regularity constraint $\frac{|\pi|}{\min_i \Delta t_i} \leq c_0$. Then there exists a constant C , independent of π , k , l , and the space dimension d , such that*

$$\begin{aligned} & \max_{0 \leq i \leq N-1} \mathbb{E} \left| u(t_i, X_{t_i}^{t,x}) - \mathcal{U}_i^*(X_{t_i}^\pi) \right|_\omega^2 \\ & \leq C \left(|\pi| + \frac{c_0}{|\pi|} \sum_{i=0}^{N-1} \left(\inf_{\theta_i} \mathbb{E} \left| \mathcal{U}_{t_i}^\pi - \mathcal{U}_i(X_{t_i}^\pi; \theta_i) \right|^2 \right) + \sum_{i=0}^{N-1} \left(\inf_{\theta_i} \mathbb{E} \left| \mathcal{V}_{t_i}^\pi - \mathcal{V}_i(X_{t_i}^\pi; \theta_i) \right|^2 \right) \right). \end{aligned}$$

Proof. From (3.9), (3.17) and (3.18), we have

$$\begin{aligned} Y_{t_i} - \mathcal{U}_{t_i}^\pi &= \mathbb{E}_i \left[Y_{t_{i+1}} - \Psi_i^*(X_{t_{i+1}}^\pi, \Delta B_i) \right] + \mathbb{E}_i \left[\int_{t_i}^{t_{i+1}} g(r, X_r, Y_r) dB_r \right] \\ & \quad + \mathbb{E}_i \left[\int_{t_i}^{t_{i+1}} f(r, X_r, Y_r, Z_r) dr - f\left(t_i, X_{t_i}^\pi, \mathcal{U}_{t_i}^\pi, \mathcal{V}_{t_i}^\pi\right) \Delta t_i \right] \\ &= \mathbb{E}_i \left[Y_{t_{i+1}} - \mathcal{U}_{i+1}^*(X_{t_{i+1}}^\pi) \right] + \mathbb{E}_i \left[\int_{t_i}^{t_{i+1}} g(r, X_r, Y_r) dB_r - g\left(t_{i+1}, X_{t_{i+1}}^\pi, \mathcal{U}_{i+1}^*(X_{t_{i+1}}^\pi)\right) \Delta B_i \right] \\ & \quad + \mathbb{E}_i \left[\int_{t_i}^{t_{i+1}} f(r, X_r, Y_r, Z_r) dr - f\left(t_i, X_{t_i}^\pi, \mathcal{U}_{t_i}^\pi, \mathcal{V}_{t_i}^\pi\right) \Delta t_i \right]. \end{aligned}$$

Using similar arguments as for Proposition 3.2 we have

$$\mathbb{E} \left| Y_{t_i} - \mathcal{U}_{t_i}^\pi \right|^2 \leq (1 + C\Delta t_i) \mathbb{E} \left| Y_{t_{i+1}} - \mathcal{U}_{i+1}^*(X_{t_{i+1}}^\pi) \right|^2 + C(1 + |x|^2)(\Delta t_i)^2.$$

It follows from the Young's inequality that

$$\begin{aligned} \mathbb{E} \left| Y_{t_i} - \mathcal{U}_i^*(X_{t_i}^\pi) \right|^2 &= \mathbb{E} \left| Y_{t_i} - \mathcal{U}_{t_i}^\pi + \mathcal{U}_{t_i}^\pi - \mathcal{U}_i^*(X_{t_i}^\pi) \right|^2 \\ &\leq (1 + \Delta t_i) \mathbb{E} \left| Y_{t_i} - \mathcal{U}_{t_i}^\pi \right|^2 + \left(1 + \frac{1}{\Delta t_i} \right) \mathbb{E} \left| \mathcal{U}_{t_i}^\pi - \mathcal{U}_i^*(X_{t_i}^\pi) \right|^2 \\ &\leq (1 + C\Delta t_i) \mathbb{E} \left| Y_{t_{i+1}} - \mathcal{U}_{i+1}^*(X_{t_{i+1}}^\pi) \right|^2 \\ &\quad + C(1 + |x|^2)(\Delta t_i)^2 + \left(1 + \frac{1}{\Delta t_i} \right) \mathbb{E} \left| \mathcal{U}_{t_i}^\pi - \mathcal{U}_i^*(X_{t_i}^\pi) \right|^2. \end{aligned}$$

Then by discrete Gronwall's inequality we obtain

$$\max_{0 \leq i \leq N-1} \mathbb{E} \left| Y_{t_i} - \mathcal{U}_i^*(X_{t_i}^\pi) \right|^2 \leq C \sum_{i=0}^{N-1} \left(1 + \frac{1}{\Delta t_i} \right) \mathbb{E} \left| \mathcal{U}_{t_i}^\pi - \mathcal{U}_i^*(X_{t_i}^\pi) \right|^2 + C(1 + |x|^2) |\pi|. \quad (3.19)$$

On the other hand by (3.18) we have

$$\begin{aligned} L_i(\theta_i) &= \mathbb{E} \left| \Psi_i^*(X_{t_{i+1}}^\pi, \Delta B_i) - \mathcal{V}_i(X_{t_i}^\pi; \theta_i) \Delta W_i + f(t_i, X_{t_i}^\pi, \mathcal{U}_i(X_{t_i}^\pi; \theta_i), \mathcal{V}_i(X_{t_i}^\pi; \theta_i)) \Delta t_i - \mathcal{U}_i(X_{t_i}^\pi; \theta_i) \right|^2 \\ &= \mathbb{E} \left| \mathcal{U}_{t_i}^\pi - f(t_i, X_{t_i}^\pi, \mathcal{U}_{t_i}^\pi, \mathcal{V}_{t_i}^\pi) \Delta t_i + \mathcal{V}_{t_i}^\pi \Delta W_i - \mathcal{V}_i(X_{t_i}^\pi; \theta_i) \Delta W_i \right. \\ &\quad \left. + f(t_i, X_{t_i}^\pi, \mathcal{U}_i(X_{t_i}^\pi; \theta_i), \mathcal{V}_i(X_{t_i}^\pi; \theta_i)) \Delta t_i - \mathcal{U}_i(X_{t_i}^\pi; \theta_i) \right|^2 \\ &= \mathbb{E} \left| \mathcal{U}_{t_i}^\pi - \mathcal{U}_i(X_{t_i}^\pi; \theta_i) \right|^2 + \Delta t_i \mathbb{E} \left| \mathcal{V}_{t_i}^\pi - \mathcal{V}_i(X_{t_i}^\pi; \theta_i) \right|^2 \\ &\quad + (\Delta t_i)^2 \mathbb{E} \left| \left(f(t_i, X_{t_i}^\pi, \mathcal{U}_i(X_{t_i}^\pi; \theta_i), \mathcal{V}_i(X_{t_i}^\pi; \theta_i)) - f(t_i, X_{t_i}^\pi, \mathcal{U}_{t_i}^\pi, \mathcal{V}_{t_i}^\pi) \right) \right|^2 \\ &\quad + 2\Delta t_i \mathbb{E} \left[\left(\mathcal{U}_{t_i}^\pi - \mathcal{U}_i(X_{t_i}^\pi; \theta_i) \right) \left(f(t_i, X_{t_i}^\pi, \mathcal{U}_i(X_{t_i}^\pi; \theta_i), \mathcal{V}_i(X_{t_i}^\pi; \theta_i)) - f(t_i, X_{t_i}^\pi, \mathcal{U}_{t_i}^\pi, \mathcal{V}_{t_i}^\pi) \right) \right] \\ &\leq (1 + \Delta t_i) \mathbb{E} \left| \mathcal{U}_{t_i}^\pi - \mathcal{U}_i(X_{t_i}^\pi; \theta_i) \right|^2 + \Delta t_i \mathbb{E} \left| \mathcal{V}_{t_i}^\pi - \mathcal{V}_i(X_{t_i}^\pi; \theta_i) \right|^2 \\ &\quad + (1 + 1/\Delta t_i)(\Delta t_i)^2 \mathbb{E} \left| \left(f(t_i, X_{t_i}^\pi, \mathcal{U}_i(X_{t_i}^\pi; \theta_i), \mathcal{V}_i(X_{t_i}^\pi; \theta_i)) - f(t_i, X_{t_i}^\pi, \mathcal{U}_{t_i}^\pi, \mathcal{V}_{t_i}^\pi) \right) \right|^2 \\ &\leq \left(1 + \Delta t_i + K\Delta t_i + K(\Delta t_i)^2 \right) \mathbb{E} \left| \mathcal{U}_{t_i}^\pi - \mathcal{U}_i(X_{t_i}^\pi; \theta_i) \right|^2 + \left(1 + K + K\Delta t_i \right) \Delta t_i \mathbb{E} \left| \mathcal{V}_{t_i}^\pi - \mathcal{V}_i(X_{t_i}^\pi; \theta_i) \right|^2. \end{aligned}$$

Notice that $2K\Delta t_i a^2 + \frac{1}{2K\Delta t_i} b^2 + 2ab = 2K\Delta t_i \left(a + \frac{1}{2K\Delta t_i} b \right)^2 \geq 0$. Thus we

have

$$\begin{aligned}
L_i(\theta_i) &\geq (1 - 2K\Delta t_i) \mathbb{E} \left| \mathcal{U}_{t_i}^\pi - \mathcal{U}_i(X_{t_i}^\pi; \theta_i) \right|^2 + \Delta t_i \mathbb{E} \left| \mathcal{V}_{t_i}^\pi - \mathcal{V}_i(X_{t_i}^\pi; \theta_i) \right|^2 \\
&\quad + \left(1 - \frac{1}{2K\Delta t_i} \right) (\Delta t_i)^2 \mathbb{E} \left| \left(f(t_i, X_{t_i}^\pi, \mathcal{U}_i(X_{t_i}^\pi; \theta_i), \mathcal{V}_i(X_{t_i}^\pi; \theta_i)) - f(t_i, X_{t_i}^\pi, \mathcal{U}_{t_i}^\pi, \mathcal{V}_{t_i}^\pi) \right) \right|^2 \\
&\geq (1 - 2K\Delta t_i) \mathbb{E} \left| \mathcal{U}_{t_i}^\pi - \mathcal{U}_i(X_{t_i}^\pi; \theta_i) \right|^2 + \Delta t_i \mathbb{E} \left| \mathcal{V}_{t_i}^\pi - \mathcal{V}_i(X_{t_i}^\pi; \theta_i) \right|^2 \\
&\quad - \frac{\Delta t_i}{2K} \mathbb{E} \left| \left(f(t_i, X_{t_i}^\pi, \mathcal{U}_i(X_{t_i}^\pi; \theta_i), \mathcal{V}_i(X_{t_i}^\pi; \theta_i)) - f(t_i, X_{t_i}^\pi, \mathcal{U}_{t_i}^\pi, \mathcal{V}_{t_i}^\pi) \right) \right|^2 \\
&\geq \left(1 - 2K\Delta t_i - \frac{1}{2}\Delta t_i \right) \mathbb{E} \left| \mathcal{U}_{t_i}^\pi - \mathcal{U}_i(X_{t_i}^\pi; \theta_i) \right|^2 + \frac{1}{2}\Delta t_i \mathbb{E} \left| \mathcal{V}_{t_i}^\pi - \mathcal{V}_i(X_{t_i}^\pi; \theta_i) \right|^2.
\end{aligned}$$

We take $\theta_i = \theta_i^*$, and it is easy to verify that

$$\left(1 - 2K\Delta t_i - \frac{1}{2}\Delta t_i \right) \mathbb{E} \left| \mathcal{U}_{t_i}^\pi - \mathcal{U}_i^*(X_{t_i}^\pi) \right|^2 \leq L_i(\theta_i^*),$$

which implies

$$\begin{aligned}
&\left(1 - 2K\Delta t_i - \frac{1}{2}\Delta t_i \right) \mathbb{E} \left| \mathcal{U}_{t_i}^\pi - \mathcal{U}_i^*(X_{t_i}^\pi) \right|^2 \\
&\leq L_i(\theta_i) \leq (1 + C\Delta t_i) \mathbb{E} \left| \mathcal{U}_{t_i}^\pi - \mathcal{U}_i(X_{t_i}^\pi; \theta_i) \right|^2 + C\Delta t_i \mathbb{E} \left| \mathcal{V}_{t_i}^\pi - \mathcal{V}_i(X_{t_i}^\pi; \theta_i) \right|^2.
\end{aligned}$$

Substituting this into the right-hand side of (3.19) yields

$$\begin{aligned}
&\max_{0 \leq i \leq N-1} \mathbb{E} \left| Y_{t_i} - \mathcal{U}_i^*(X_{t_i}^\pi) \right|^2 \\
&\leq C \sum_{i=0}^{N-1} \left(\frac{c_0}{|\pi|} \mathbb{E} \left| \mathcal{U}_{t_i}^\pi - \mathcal{U}_i(X_{t_i}^\pi; \theta_i) \right|^2 + \mathbb{E} \left| \mathcal{V}_{t_i}^\pi - \mathcal{V}_i(X_{t_i}^\pi; \theta_i) \right|^2 \right) \\
&\quad + C(1 + |x|^2)|\pi|.
\end{aligned} \tag{3.20}$$

Consequently, we have

$$\begin{aligned}
&\max_{0 \leq i \leq N-1} \mathbb{E} |Y_{t_i} - \mathcal{U}_i^*(X_{t_i}^\pi)|^2 \\
&\leq C \sum_{i=0}^{N-1} \left(\frac{c_0}{|\pi|} \inf_{\theta_i} \mathbb{E} \left| \mathcal{U}_{t_i}^\pi - \mathcal{U}_i(X_{t_i}^\pi; \theta_i) \right|^2 + \inf_{\theta_i} \mathbb{E} \left| \mathcal{V}_{t_i}^\pi - \mathcal{V}_i(X_{t_i}^\pi; \theta_i) \right|^2 \right) \\
&\quad + C(1 + |x|^2)|\pi|.
\end{aligned}$$

The desired result follows by using an similar argument as in the proof of Theorem 3.3. The proof is complete. \square

Theorem 3.4 indicates that the approximation error of the proposed algorithm can be controlled by the neural network approximation errors $\mathbb{E} |\mathcal{U}_{t_i}^\pi - \mathcal{U}_i(X_{t_i}^\pi; \theta_i)|^2$ and $\mathbb{E} |\mathcal{V}_{t_i}^\pi - \mathcal{V}_i(X_{t_i}^\pi; \theta_i)|^2$. In addition, the number of parameters $n_{\mathcal{W}}$ used in the neural network grows at most polynomially in the space dimension d , similar as in [36].

4 Numerical examples

In this section, we shall present some numerical experiments. All our numerical tests are performed in Python using TensorFlow 2.7 on a laptop equipped with an Intel Core i5 Processor with 1.8GHz. We use fully connected layers and batch normalization [37] after each matrix multiplication and before activation. We employ the Leaky Rectified Linear Unit function as the activation function for the hidden layers, and the identity function as the activation function for the output layer. For the optimization solver, we use Adam optimizer [41] with the exponential decay rate of 0.9 for the first moment estimates, and the exponential decay rate of 0.999 for the second moment estimates. The training was on mini-batches with 64 trajectories of X per batch for 100 epochs. All the weights in the network are initialized using the He initialization method [31]. We use adaptive learning rate for the training process with a starting value of 0.01 and drop it by half if the loss doesn't decrease for 10 consecutive epochs.

We consider an example adapted from Section 4 in [56], for which the parameters of the SPDE (1.1) are chosen as: $k = 1$, $l = 1$, $\sigma = 0.25$, $T = 1$, $\mu(t, x) = \sigma\sqrt{d}\sin(x)$, $\sigma(t, x) = \sigma\sqrt{d}I_d$, $h(x) = \sqrt{d}\arctan(\frac{1}{d}\sum_{j=1}^d x_j) + \frac{\pi}{2}\sqrt{d}$, $f = -\sigma\sin(x)\nabla u$, and $g = -\sigma\sqrt{d}\sin^2(\frac{1}{\sqrt{d}}u)$. We also set $X_0 \sim U(-0.2, 0.2)$ to avoid overfitting. The associated exact solution reads:

$$u(t, X_t) = \sqrt{d}\arctan\left(\frac{1}{d}\sum_{j=1}^d(X_t)_j - \sigma(B_T - B_t)\right) + \frac{\pi}{2}\sqrt{d}.$$

We shall test our algorithm in four cases: the one-dimensional case, a moderate dimensional (5-dimensional) case, and two high-dimensional (50 and 100-dimensional) cases.

For the one-dimensional case, we discretize the equation using $N = 32$ time steps. Each of the neural networks consists of 2 hidden layers with 11 nodes. The number of iterations per epoch is set to be 100. The simulation results are presented in Table 1. For each fixed sample path of B , we provide the average $\bar{\mathcal{U}}_0^*(X_0^\pi)$ and the standard deviation of $\mathcal{U}_0^*(X_{t_0}^\pi)$ by performing 5 independent runs of the algorithm. The relative error is calculated as

$$\frac{|\bar{\mathcal{U}}_0^*(X_{t_0}^\pi) - u(0, X_0)|}{u(0, X_0)}.$$

We show in Figs.1-5 a comparison between the exact solution and the approximate solutions at $t = 0.03125$ for each realization of B . The approximation errors are also presented in Table 1. It is clearly shown that the numerical solution match well with the exact solution.

Averaged Approx.	Exact solution	Standard deviation	Relative error
1.5998764	1.596926235	0.004728534	0.001847402
1.9575781	1.967079301	0.002868398	0.004830106
1.8510513	1.847140899	0.001399888	0.002117002
1.8063872	1.808914966	0.004120083	0.001397394
1.4118652	1.403613807	0.00232844	0.005878677
Relative L^2 error: 0.00368065398642483			

Table 1: Numerical results for the one-dimensional case

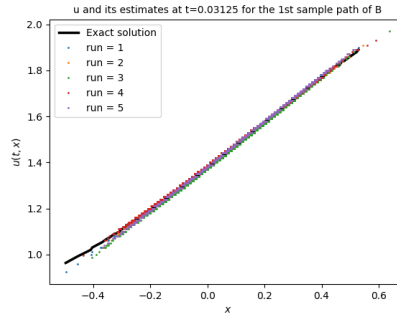


Figure 1: Comparison between the exact solution and the approximate solutions for the 1st sample path of B ($d = 1$)

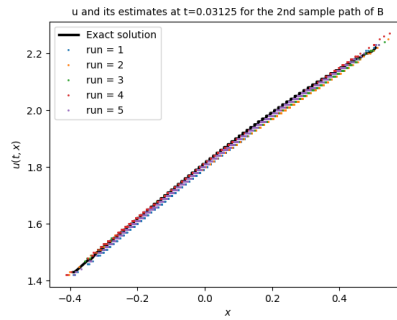


Figure 2: Comparison between the exact solution and the approximate solutions for the 2nd sample path of B ($d = 1$)

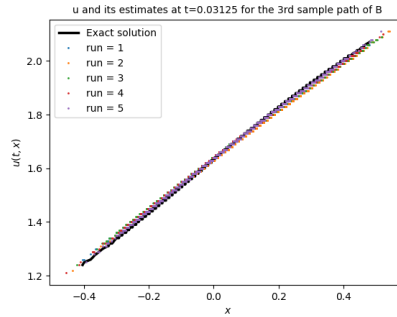


Figure 3: Comparison between the exact solution and the approximate solutions for the 3rd sample path of B ($d = 1$)

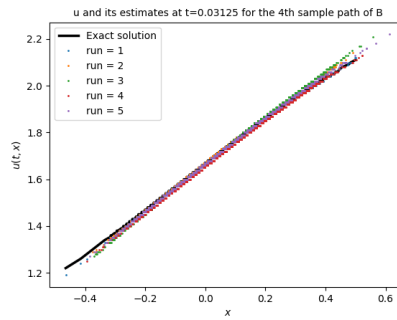


Figure 4: Comparison between the exact solution and the approximate solutions for the 4th sample path of B ($d = 1$)

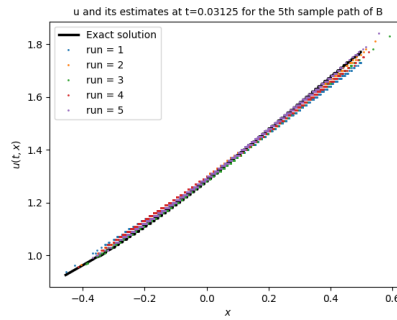


Figure 5: Comparison between the exact solution and the approximate solutions for the 5th sample path of B ($d = 1$)

Similarly, numerical results for the 5-dimensional, 50-dimensional and 100-dimensional cases are given in Tables 2-4, respectively. For these cases, the number of time steps is set to be 16. Each of the neural networks consists of 2 hidden layers, the number of nodes for each hidden layer is set to be $d+10$ for 5-dimensional case, and $d+50$ for 50- and 100-dimensional cases. To illustrate the accuracy of the proposed algorithm, we also plot in Figures 6-10 the comparison between exact solution and the approximation solution of the 100-dimensional case as a function of $\frac{1}{100} \sum_{j=1}^{100} (X_t)_j$ at $t = 0.0625$ for each realization of B in Table 4.

Averaged Approx.	Exact solution	Standard deviation	Relative error
3.7816436	3.783391082	0.01756304	0.000461883
4.0550942	4.092778688	0.01245616	0.009207556
3.5838552	3.589354974	0.025385832	0.001532246
3.9931598	4.034977758	0.03498262	0.010363863
3.6655762	3.675363075	0.006242963	0.002662832
Relative L^2 error: 0.00635359012791855			

Table 2: Numerical results for the 5-dimensional case.

Averaged Approx.	Exact solution	Standard deviation	Relative error
13.869227	13.80994108	0.0389653	0.004292989
11.789759	11.77779362	0.026603295	0.001015927
11.142225	11.12731684	0.02187582	0.00133978
8.79433	8.691944684	0.0351124	0.011779334
8.846188	8.819915756	0.02828248	0.002978741
Relative L^2 error: 0.00581175481223784			

Table 3: Numerical results for the 50-dimensional case.

Averaged Approx.	Exact solution	Standard deviation	Relative error
13.589519	13.50290922	0.06967104	0.006414157
10.588926	10.61844227	0.061020687	0.002779717
19.077723	18.69746132	0.048847217	0.02033761
14.551335	14.54826577	0.023958674	0.000210969
17.445202	17.53231125	0.022984497	0.004968498
Relative L^2 error: 0.00987134339284379			

Table 4: Numerical results for the 100-dimensional case.

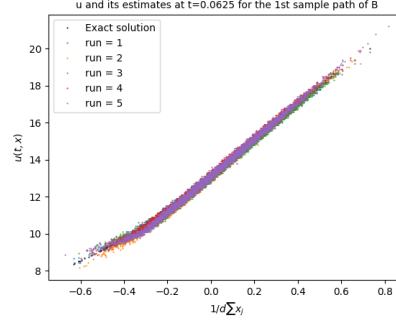


Figure 6: Comparison between the exact solution and the approximate solutions for the 1st sample path of B ($d = 100$)

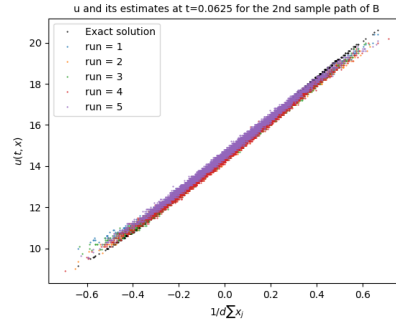


Figure 7: Comparison between the exact solution and the approximate solutions for the 2nd sample path of B ($d = 100$)

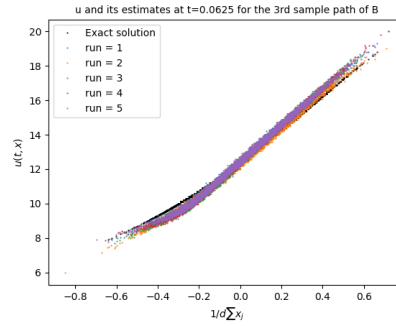


Figure 8: Comparison between the exact solution and the approximate solutions for the 3rd sample path of B ($d = 100$)

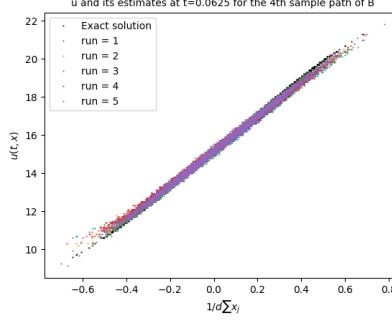


Figure 9: Comparison between the exact solution and the approximate solutions for the 4th sample path of B ($d = 100$)

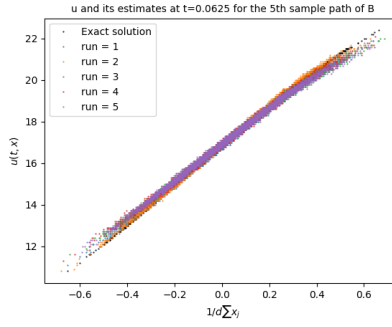


Figure 10: Comparison between the exact solution and the approximate solutions for the 5th sample path of B ($d = 100$)

5 Conclusions

We have proposed a predictor-corrector deep learning-based numerical method for solving high dimensional stochastic partial differential equations. At each time step, the original SPDE is first decomposed into a degenerate SPDE to serve as the prediction step, and a second-order deterministic PDE to serve as the correction step. The solution of the degenerate SPDE is then approximated by the Euler method, and the solution of the PDE is approximated by deep neural networks via the equivalent backward stochastic differential equation. The convergence analysis of the proposed algorithm is presented, and numerical examples are carried out to show the efficiency of the proposed algorithm. Future studies along this line include extending the current algorithm to solve nonlinear SPDEs and stochastic optimal control involving SPDEs.

References

- [1] Richard Archibald, Feng Bao, Yanzhao Cao, and He Zhang. A backward sde method for uncertainty quantification in deep learning. *Discrete and Continuous Dynamical Systems - S*, 15(10):2807–2835, 2022.
- [2] Achref Bachouch, Mohamed Anis Ben Lasmar, Anis Matoussi, and Mohamed Mnif. Euler time discretization of backward doubly SDEs and application to semilinear SPDEs. *Stoch. Partial Differ. Equ. Anal. Comput.*, 4(3):592–634, 2016.
- [3] Achref Bachouch, Emmanuel Gobet, and Anis Matoussi. Empirical regression method for backward doubly stochastic differential equations. *SIAM/ASA J. Uncertain. Quantif.*, 4(1):358–379, 2016.
- [4] Vlad Bally and Anis Matoussi. Weak solutions for SPDEs and backward doubly stochastic differential equations. *J. Theoret. Probab.*, 14(1):125–164, 2001.
- [5] Feng Bao, Yanzhao Cao, and Weidong Zhao. A first order semi-discrete algorithm for backward doubly stochastic differential equations. *Discrete Contin. Dyn. Syst. Ser. B*, 20(5):1297–1313, 2015.
- [6] Christian Beck, Sebastian Becker, Patrick Cheridito, Arnulf Jentzen, and Ariel Neufeld. Deep learning based numerical approximation algorithms for stochastic partial differential equations and high-dimensional nonlinear filtering problems. *arXiv preprint arXiv:2012.01194*, 2020.
- [7] Christian Beck, Weinan E, and Arnulf Jentzen. Machine learning approximation algorithms for high-dimensional fully nonlinear partial differential equations and second-order backward stochastic differential equations. *J. Nonlinear Sci.*, 29(4):1563–1619, 2019.
- [8] Alain Bensoussan and Roland Glowinski. Approximation of Zakai equation by the splitting up method. In *Stochastic systems and optimization (Warsaw, 1988)*, volume 136 of *Lect. Notes Control Inf. Sci.*, pages 257–265. Springer, Berlin, 1989.
- [9] Alain Bensoussan, Roland Glowinski, and Aurel Răşcanu. Approximation of the Zakai equation by the splitting up method. *SIAM J. Control Optim.*, 28(6):1420–1431, 1990.
- [10] Alain Bensoussan, Roland Glowinski, and Aurel Răşcanu. Approximation of some stochastic differential equations by the splitting up method. *Appl. Math. Optim.*, 25(1):81–106, 1992.
- [11] Bruno Bouchard and Nizar Touzi. Discrete-time approximation and Monte-Carlo simulation of backward stochastic differential equations. *Stochastic Process. Appl.*, 111(2):175–206, 2004.

- [12] Sonja Cox and Jan van Neerven. Convergence rates of the splitting scheme for parabolic linear stochastic Cauchy problems. *SIAM J. Numer. Anal.*, 48(2):428–451, 2010.
- [13] Giuseppe Da Prato, Arnulf Jentzen, and Michael Röckner. A mild Itô formula for SPDEs. *Trans. Amer. Math. Soc.*, 372(6):3755–3807, 2019.
- [14] Weinan E. A proposal on machine learning via dynamical systems. *Commun. Math. Stat.*, 5(1):1–11, 2017.
- [15] Weinan E. Machine learning and computational mathematics. *Commun. Comput. Phys.*, 28(5):1639–1670, 2020.
- [16] Weinan E, Jiequn Han, and Arnulf Jentzen. Deep learning-based numerical methods for high-dimensional parabolic partial differential equations and backward stochastic differential equations. *Commun. Math. Stat.*, 5(4):349–380, 2017.
- [17] Weinan E, Jiequn Han, and Arnulf Jentzen. Algorithms for solving high dimensional PDEs: from nonlinear Monte Carlo to machine learning. *Nonlinearity*, 35(1):278–310, 2022.
- [18] Weinan E, Martin Hutzenthaler, Arnulf Jentzen, and Thomas Kruse. On multilevel Picard numerical approximations for high-dimensional nonlinear parabolic partial differential equations and high-dimensional nonlinear backward stochastic differential equations. *J. Sci. Comput.*, 79(3):1534–1571, 2019.
- [19] Xiaodong Feng, Li Zeng, and Tao Zhou. Solving time dependent Fokker-Planck equations via temporal normalizing flow. *Commun. Comput. Phys.*, 32(2):401–423, 2022.
- [20] Yu Fu, Weidong Zhao, and Tao Zhou. Efficient spectral sparse grid approximations for solving multi-dimensional forward backward SDEs. *Discrete Contin. Dyn. Syst. Ser. B*, 22(9):3439–3458, 2017.
- [21] Maximilien Germain, Huyên Pham, and Xavier Warin. Approximation error analysis of some deep backward schemes for nonlinear PDEs. *SIAM J. Sci. Comput.*, 44(1):A28–A56, 2022.
- [22] Alfredo Germani and Mauro Piccioni. Semidiscretization of stochastic partial differential equations on \mathbf{R}^d by a finite-element technique. *Stochastics*, 23(2):131–148, 1988.
- [23] Emmanuel Gobet, Jean-Philippe Lemor, and Xavier Warin. A regression-based Monte Carlo method to solve backward stochastic differential equations. *Ann. Appl. Probab.*, 15(3):2172–2202, 2005.
- [24] Emmanuel Gobet and Plamen Turkedjiev. Approximation of backward stochastic differential equations using Malliavin weights and least-squares regression. *Bernoulli*, 22(1):530–562, 2016.

- [25] Emmanuel Gobet and Plamen Turkedjiev. Linear regression MDP scheme for discrete backward stochastic differential equations under general conditions. *Math. Comp.*, 85(299):1359–1391, 2016.
- [26] Wilfried Grecksch and Peter E. Kloeden. Time-discretised Galerkin approximations of parabolic stochastic PDEs. *Bull. Austral. Math. Soc.*, 54(1):79–85, 1996.
- [27] István Gyöngy and Nicolai Krylov. On the splitting-up method and stochastic partial differential equations. *Ann. Probab.*, 31(2):564–591, 2003.
- [28] István Gyöngy and Nicolai Krylov. Accelerated finite difference schemes for linear stochastic partial differential equations in the whole space. *SIAM J. Math. Anal.*, 42(5):2275–2296, 2010.
- [29] István Gyöngy and David Nualart. Implicit scheme for stochastic parabolic partial differential equations driven by space-time white noise. *Potential Anal.*, 7(4):725–757, 1997.
- [30] Jiequn Han, Arnulf Jentzen, and Weinan E. Solving high-dimensional partial differential equations using deep learning. *Proc. Natl. Acad. Sci. USA*, 115(34):8505–8510, 2018.
- [31] Kaiming He, Xiangyu Zhang, Shaoqing Ren, and Jian Sun. Delving deep into rectifiers: Surpassing human-level performance on imagenet classification. In *Proceedings of the IEEE International Conference on Computer Vision (ICCV)*, December 2015.
- [32] Pierre Henry-Labordère, Nadia Oudjane, Xiaolu Tan, Nizar Touzi, and Xavier Warin. Branching diffusion representation of semilinear PDEs and Monte Carlo approximation. *Ann. Inst. Henri Poincaré Probab. Stat.*, 55(1):184–210, 2019.
- [33] Yaozhong Hu, David Nualart, and Xiaoming Song. An implicit numerical scheme for a class of backward doubly stochastic differential equations. *Stochastic Process. Appl.*, 130(6):3295–3324, 2020.
- [34] Jianguo Huang, Haoqin Wang, and Tao Zhou. An augmented Lagrangian deep learning method for variational problems with essential boundary conditions. *Commun. Comput. Phys.*, 31(3):966–986, 2022.
- [35] Côme Huré, Huyên Pham, and Xavier Warin. Deep backward schemes for high-dimensional nonlinear PDEs. *Math. Comp.*, 89(324):1547–1579, 2020.
- [36] Martin Hutzenthaler, Arnulf Jentzen, Thomas Kruse, and Tuan Anh Nguyen. A proof that rectified deep neural networks overcome the curse of dimensionality in the numerical approximation of semilinear heat equations. *Partial Differ. Equ. Appl.*, 1(2):Paper No. 10, 34, 2020.

- [37] Sergey Ioffe and Christian Szegedy. Batch normalization: Accelerating deep network training by reducing internal covariate shift. In Francis Bach and David Blei, editors, *Proceedings of the 32nd International Conference on Machine Learning*, volume 37 of *Proceedings of Machine Learning Research*, pages 448–456, Lille, France, 07–09 Jul 2015. PMLR.
- [38] Arnulf Jentzen and Peter E. Kloeden. The numerical approximation of stochastic partial differential equations. *Milan J. Math.*, 77:205–244, 2009.
- [39] Arnulf Jentzen and Peter E. Kloeden. Taylor expansions of solutions of stochastic partial differential equations with additive noise. *Ann. Probab.*, 38(2):532–569, 2010.
- [40] Arnulf Jentzen and Michael Röckner. A Milstein scheme for SPDEs. *Found. Comput. Math.*, 15(2):313–362, 2015.
- [41] Diederik P. Kingma and Jimmy Ba. Adam: A method for stochastic optimization. In Yoshua Bengio and Yann LeCun, editors, *3rd International Conference on Learning Representations, ICLR 2015, San Diego, CA, USA, May 7-9, 2015, Conference Track Proceedings*, 2015.
- [42] Peter E. Kloeden and Eckhard Platen. *Numerical solution of stochastic differential equations*, volume 23 of *Applications of Mathematics (New York)*. Springer-Verlag, Berlin, 1992.
- [43] Nicolai Krylov and Boris Rozovskii. Stochastic evolution equations. In *Stochastic differential equations: theory and applications*, volume 2 of *Interdiscip. Math. Sci.*, pages 1–69. World Sci. Publ., Hackensack, NJ, 2007.
- [44] François Le Gland. Splitting-up approximation for SPDEs and SDEs with application to nonlinear filtering. In *Stochastic partial differential equations and their applications (Charlotte, NC, 1991)*, volume 176 of *Lect. Notes Control Inf. Sci.*, pages 177–187. Springer, Berlin, 1992.
- [45] Sergey Vladimir Lototsky. *Problems in statistics of stochastic differential equations*. ProQuest LLC, Ann Arbor, MI, 1996. Thesis (Ph.D.)—University of Southern California.
- [46] Jin Ma and Jiongmin Yong. *Forward-backward stochastic differential equations and their applications*, volume 1702 of *Lecture Notes in Mathematics*. Springer-Verlag, Berlin, 1999.
- [47] Jin Ma and Jianfeng Zhang. Representation theorems for backward stochastic differential equations. *Ann. Appl. Probab.*, 12(4):1390–1418, 2002.
- [48] Grigori Milstein and Michael Tretyakov. Solving parabolic stochastic partial differential equations via averaging over characteristics. *Math. Comp.*, 78(268):2075–2106, 2009.

- [49] Noriaki Nagase. Remarks on nonlinear stochastic partial differential equations: an application of the splitting-up method. *SIAM J. Control Optim.*, 33(6):1716–1730, 1995.
- [50] Étienne Pardoux and Shige Peng. Backward stochastic differential equations and quasilinear parabolic partial differential equations. In *Stochastic partial differential equations and their applications (Charlotte, NC, 1991)*, volume 176 of *Lect. Notes Control Inf. Sci.*, pages 200–217. Springer, Berlin, 1992.
- [51] Étienne Pardoux and Shige Peng. Backward doubly stochastic differential equations and systems of quasilinear SPDEs. *Probab. Theory Related Fields*, 98(2):209–227, 1994.
- [52] Huy  n Pham, Xavier Warin, and Maximilien Germain. Neural networks-based backward scheme for fully nonlinear PDEs. *Partial Differ. Equ. Appl.*, 2(1):Paper No. 16, 24, 2021.
- [53] M. Raissi, P. Perdikaris, and G. E. Karniadakis. Physics-informed neural networks: a deep learning framework for solving forward and inverse problems involving nonlinear partial differential equations. *J. Comput. Phys.*, 378:686–707, 2019.
- [54] Maziar Raissi. Forward-backward stochastic neural networks: Deep learning of high-dimensional partial differential equations. *arXiv preprint arXiv:1804.07010*, 2018.
- [55] Justin Sirignano and Konstantinos Spiliopoulos. DGM: a deep learning algorithm for solving partial differential equations. *J. Comput. Phys.*, 375:1339–1364, 2018.
- [56] Bin Teng, Yufeng Shi, and Qingfeng Zhu. Solving high-dimensional forward-backward doubly SDEs and their related SPDEs through deep learning. *Personal and Ubiquitous Computing*, pages 1–8, 2021.
- [57] John Bradstreet Walsh. Finite element methods for parabolic stochastic PDE’s. *Potential Anal.*, 23(1):1–43, 2005.
- [58] Jie Yang, Weidong Zhao, and Tao Zhou. A unified probabilistic discretization scheme for FBSDEs: stability, consistency, and convergence analysis. *SIAM J. Numer. Anal.*, 58(4):2351–2375, 2020.
- [59] Hyek Yoo. Semi-discretization of stochastic partial differential equations on \mathbf{R}^1 by a finite-difference method. *Math. Comp.*, 69(230):653–666, 2000.
- [60] Jianfeng Zhang. A numerical scheme for BSDEs. *Ann. Appl. Probab.*, 14(1):459–488, 2004.
- [61] Weidong Zhao, Jinlei Wang, and Shige Peng. Error estimates of the θ -scheme for backward stochastic differential equations. *Discrete Contin. Dyn. Syst. Ser. B*, 12(4):905–924, 2009.